HHS Public Access

Author manuscript

Eur Respir J. Author manuscript; available in PMC 2020 August 15.

Published in final edited form as:

Eur Respir J. 2019 August ; 54(2): . doi:10.1183/13993003.00370-2019.

Pulmonary Vascular Density: Comparison of Findings on CT Imaging with Histology.

Farbod N. Rahaghi[*,1,Δ], **Gemma Argemí**[*,2], **Pietro Nardelli**[3], **David Domínguez-Fandos**[2], **Pedro Arguis**[4], **Víctor I. Peinado**[2,5], **James C. Ross**[3], **Samuel Ash**[1], **Isaac de La Bruere**[1], **Carolyn E. Come**[1], **Alejandro A. Diaz**[1], **Marcelo Sánchez**[4], **George R. Washko**[1,++], **Joan Albert Barberà**[2,5,++], **Raúl San José Estépar**[1,++]

[1]Brigham and Women's Hospital, Pulmonary and Critical Care Division of Department of Medicine 75 Francis Street, PBB – CA 3 Boston, MA 02115.

[2]Department of Pulmonary Medicine, Hospital Clínic-IDIBAPS, University of Barcelona, Barcelona, Spain.

[3]Department of Radiology, Harvard School of Medicine.

[4]Department of Radiology, Hospital Clínic-IDIBAPS, University of Barcelona, Barcelona, Spain.

[5]Biomedical Research Networking Center for Respiratory Diseases (CIBERES), Madrid, Spain.

Abstract

Background & Significance: Exposure to cigarette smoke has been shown to lead to vascular remodeling. CT-imaging measures of vascular pruning have been associated with pulmonary vascular disease, an important morbidity associated with smoking. In this study we compare CT-based measures of distal vessel loss to histologic vascular and parenchymal changes.

Methods: A retrospective review of 80 patients having undergone lung resection identified patients with imaging appropriate for 3D vascular reconstruction (N=18) and a second group for 2D analysis (N=19). Measurement of the volume of the small vessels (3D) and the cross-sectional area of small vessels (<5mm^2 cross-section) were computed. Histologic measures of cross-sectional area of the vasculature and loss of alveoli septa were obtained for all subjects.

Results: The 2D Cross-sectional area of the vasculature on CT imaging was associated with the histological vascular cross-sectional area (R=0.69; p=0.001). The arterial small vessel volume assessed by CT scan correlated with histological vascular cross-sectional area (Spearman R=0.50; p=0.04), a relationship which persisted even when adjusted for CT derived measure of emphysema in a regression model.

Conclusions: Loss of small vessel volume in CT imaging of smokers is associated with histologic loss of vascular cross sectional area. Imaging based quantification of pulmonary vasculature provides a non-invasive method to study the multi-scale effects of smoking on the pulmonary circulation.

[Δ]To whom correspondence should be addressed.
[*]Equal contributors on this manuscript
[++]Equal contributors on this manuscript

Introduction

Chronic exposure to cigarette smoke can result in emphysematous destruction of the lung parenchyma, inflammation, destruction of the airways, and remodeling of the pulmonary vasculature (1, 2). While some smokers suffering from the latter process may develop overt pulmonary hypertension (3–6), pulmonary vascular remodeling in smokers may be an integral part of the pathway from lung health to advanced disease (7–10). As such, histologic and imaging based metrics of this process may provide useful features for detecting susceptibility to disease and stratifying its severity.

Remodeling of the pulmonary vasculature has been observed on histologic and in-vivo image based investigations (2, 7, 11–16). These studies have demonstrated that the loss of micro vasculature is associated with the loss of alveolar septa, characteristic of emphysema (11, 17). In clinical investigations, quantitative measures of small vessel cross sectional area have been shown to be related to multiple parameters of smoking-related pulmonary vascular disease severity (11, 12, 18, 19). There is little data, however, linking histopathologic data to those obtained from computed tomography (CT) scan.

In this study we sought to determine the relationship between CT based measures of small vessel volume and the loss of micro-vasculature on histologic examination. We hypothesized that small vessel loss on CT was related to microvascular pruning. Establishing such a link would further substantiate CT measures of the pulmonary vasculature as providing insight to lung pathology in smokers.

Methods

Subject Selection

Subjects from Hospital Clínic of Barcelona were selected by review of CT scans in a prospective cohort of 80 subjects that had undergone surgical lung resection for lung cancer, for which histologic samples had been acquired and processed as part of a study of histology in smokers. The study was approved by the Ethics Committee of Hospital Clínic (RE 2012/7982) and all subjects provided written informed consent to participate in the study. Two cohorts were selected with no overlap between the two cohorts. The first cohort had CT scans with thin sections sufficient for 3D reconstruction (1.0–1.5mm in thickness) obtained using the same scanner (Siemens Emotion 16) with similar reconstruction kernels (B30s, B31s and B41s). This constituted the 3D analysis cohort. The second cohort consisted of subjects possessing CT scans with similar reconstruction kernels (B70, B75, B80) and thickness between 1– 2mm (mostly 2mm) but to which a 2D measure of small vessel density would be then applied. Criteria for exclusion included poor quality due to motion artifact, missing part of the scan, or significant infiltrates in the lung resected that would confound analysis. Characteristics of the subjects in the two cohorts are shown in Table 1.

Histologic Processing

Lung tissue samples were collected prospectively and processed after surgery. Part of the histological samples had been stored at the Hospital Clínic of Barcelona Core of the Pulmonary Biobank Consortium of the Biomedical Research Networking Center for

Respiratory Diseases (CIBERES). Briefly, immediately to resection, fresh lung tissue slices of 3–4 mm thick were washed 3 times (10 min each) in cold PBS in order to distend collapsed areas of parenchyma and clean of embedded blood. Paraffin embedded lung tissue blocks were sectioned into 5 μm thick slices that were stained with Hematoxilin and Eosin (H&E). Slices were imaged at 40× magnification using a bright field microscope (model DM 5000) connected to a Leica camera (model DFC 500) (Leica Microsystems, Wetzlar, Germany). Four images per subject were acquired and analyzed with the ImagePro software. The cross-sectional area (CSA) of vessels <500 μm in diameter was manually calculated and expressed as a percent of the total area of the four lung tissue images (%hist-VCSA) (Figure 1). Vessels with a diameter ≥500 μm or with a longitudinal disposition (ratio major/minor diameter >2:1) were discarded. The proportions of lung tissue structures (alveolar septa, vessels and bronchioles) were estimated by using a point counting method. To this end, a grid with 108 intersection points was superimposed on the microscopic field at a 40× magnification and each intersection point was assigned to alveolar septum, vessel, bronchiole or airspace. Counts superimposed on each structure were then divided by the total number of points on the grid and expressed as a percentage (Figure 1). Ten pulmonary muscular arteries per subject were identified and the external and internal elastic laminas and the inner aspect of the intima were outlined. The areas occupied by the muscular layer, the intimal layer and the lumen were computed and expressed as a percentage of the measured total area. Visual example of these processes are shown in Figure 1.

Computed Tomographic Vascular Analysis

2D Analysis—Cross sectional area of vasculature was computed as previously described using Image J version 1.46r (20). A visual example of this process is shown in Figure S-1. In summary, circle-like objects with an area of less than $5mm^2$ were identified on an individual slice; the aggregate area of these were then divided by the lung CSA in the same slice yielding the CSA5%. 2D analysis was performed in the same side as the histologic sample. For patients with upper lobe resections or pneumonectomies, a section at the same level as the aortic arch was used. For those with lower lobe resections, a CT Slice at the level of the carina was used. Images were not blurred prior to analysis.

3D Analysis—The lungs were automatically segmented from the chest wall and 3D reconstructions of the vasculature were created (21–23) for the entirety of the lung. The vessel size estimation was performed with a deep learning based approach which used generative models of the vessel, estimating radius from images in the orthogonal plane of the vessel (24). The volume of vasculature was computed as a function of CSA of the vessels and the total volume in small vessels was derived and termed BV5 - a cutoff of $5mm^2$ was used consistent with prior investigations. BV5 was divided by the volume of the lung to arrive at a vascular density (BV5/LV). As hyperinflation of the lung can confound the use of lung volume in smokers, a nonemphysematous lung volume was also computed using the following equation:

$$\text{Non-Emphysematous Lung Volume} = \text{Lung Volume} - \text{Total Vessel Volume} - \text{Volume of Emphysema} \quad (1)$$

The volume of emphysematous tissue was computed using the measurement of percentage of voxels that fell below -950 Hounsfield Units (LAA-950), as previously described (25, 26). This was then used to arrive at a second normalized measure of small vessel volume, BV5/NELV.

Automated Arterial/Venous (AV) segmentation was performed using a convolutional neural network algorithm previously described(27). In order to validate this method in this cohort, six cases were randomly selected and reviewed by tracing the path of the vessels from their origins to the pulmonary artery and the left atrium. Disagreements between the automated and manual method were measured segment by segment. The blood vessel volumes were then computed separately for the arterial and venous vasculature.

Statistical analysis

Data are presented as means and standard deviations. All statistical analyses were performed using R 3.5. Correlations were evaluated using Pearson and Spearman correlation when appropriate. P values less than 0.05 were considered statistically significant.

Results

From a total of 80 subjects with appropriate histologic samples, 18 subjects were identified with adequate imaging for 3D reconstruction and 19 subjects were identified for 2D vascular analysis. The demographics, smoking history and pulmonary function test results for these subjects are shown in Tables 1 and S1. Tables 2 and S2 show the results of the histologic assessments.

Volumetric reconstructions of the pulmonary vasculature were performed in each subject. An example of two different 3D reconstructions with low and high BV5/LV are shown in Figure 2. The CT-derived vascular ratios (BV5/LV, BV5/NELV) that describe vascular density changes are summarized in Table 3.

The relationships between imaging and histologic metrics of septal and vascular densities in the 2D cohort are shown in Figure 3. There was a significant positive correlation (R=0.69, p=0.001) between %hist-VCSA and CSA5%. In addition, CSA5% was positively correlated with the estimated proportion of alveolar septa (R=0.57, p=0.01).

Arterial/Venous segmentation was performed successfully for all 3D cases and comparison with manual segmentation in six randomly selected cases yielded an agreement of 96.7%. An example of an AV segmentation is shown in Figure 4. Given a number of outlying points, nonparametric (spearman) correlation was used to evaluate the relationship between arterial small vessel volume (aBV5/LV) and %hist-VCSA. There was a statistically significant relationship between aBV5/LV and %hist-VCSA (R = 0.50, p = 0.04) which was not observed in the venous counterpart (vBV5/LV) (R= 0.10; p = 0.70), as shown in Figure 5. Additionally, there was a relationship between arterial/venous small vessel volume and percentage of alveolar septa, though this only reached statistical significance for venous proportion (arterial BV5/LV R = 0.41, p = 0.09; venous BV5/LV R = 0.54, p = 0.02). Normalization by non-emphysematous lung volume (NELV) altered the correlations slightly

(Arterial: R = 0.47, p = 0.05; Venous R = 0.10, p = 0.70). In combining the two arterial and venous measures, there was a direct correlation between increasing BV5/LV and percentage of alveolar septa (R = 0.54, p = 0.02); However, the correlation with %hist-VCSA was no longer significant (R = 0.18, p = 0.48).

In looking at specific arterial CT measures and evidence of arterial remodeling as measured by vessel morphometry, there was a negative correlation between aBV5/LV and %Lumen Area (R = -0.54, p = 0.02) and a positive correlation with %Intima Area (R = 0.48, p = 0.04). The relationship between arterial small vessel volume (aBV5_LV) with %hist-VCSA was further explored with a linear regression model, adjusted for CT based measure of emphysema (%LAA-950). In this model, increased distal arterial volume (aBV5_LV) remained a positive predictor of histologic vascular cross-sectional area (%hist-VCSA) even when adjusted for estimated emphysema obtained from the same CT scan (Effect Estimate 0.0005, SE 0.0001, p = 0.001, Model R^2 = 0.51).

Discussion

The goal of this study was to examine the relationship between CT based markers of small vessel loss (“pruning”) and the histologic evidence of such vessel loss. In subjects with CT scans that allowed 3D vascular reconstruction (3D cohort), we accomplished this by using CT derived measures of small vessel volume normalized either by lung volume or by the non-vascular non-emphysematous tissue volume (arterial and venous BV5/LV and BV5/NELV, respectively). In a separate series of subjects with thin enough sections and uniform image type (but not high quality enough for 3D reconstruction), we performed a 2D equivalent of this method where the vascular CSA was divided by lung slice area (CSA5%). A histologic equivalent to these measures was proposed and measured, in which the CSA of vessels <500 μm of diameter was divided by the total area of the tissue being examined, as well as the estimated proportion of alveolar septa in lung tissue. In both analyses, imaging based markers of small vessel volume loss correlated with their histologic counterparts, and were also related to measures of alveolar destruction (presence/absence of alveolar septa).

While tissue destruction due to emphysema is one mechanism of vascular impairment in smokers, multiple other pathways including those modulated by inflammatory mediators, vessel remodeling, hypoxic vasoconstriction and compression due to air-trapping have been described in leading to pulmonary vascular disease. In addition, multiple cardiovascular comorbidities exist which confound smoking exposure and may also affect the pulmonary vasculature (for example as is the case in left sided heart failure). In our study, we observed these comorbidities in 6 subjects (31.5%) in the 2D cohort and 12 subjects (67%) in the 3D cohort. The degree to which each of these mechanisms affects the micro (apparent on histology) and macro (apparent on CT) vasculature is unknown.

This study shows that there is a relationship between changes of vascular density as assessed by histology and as measured by CT scans. This relationship may be partially mediated by alveolar destruction as evidenced by correlations with proportion of alveolar septa. The %LAA-950 when added to a predictive model of the tissue vascular density did not eliminate the predictive power of aBV5/LV). It should be noted that in this cohort of patients

candidates to lung resection with normal or only mildly impaired pulmonary function, the extent of emphysema visible on CT scan as assessed by %LAA-950 was small (Table 3), suggesting that microscopic alveolar destruction might be present before CT evidence of emphysema is apparent. Examining the relationship between vascular changes in histology and those noted on imaging may improve our understanding of the role of the vasculature in the progression of lung disease in smokers.

Interestingly, measurements of arterial small vessel density (aBV5/LV) did correlate with morphometric assessments of vessel remodeling in pulmonary muscular arteries. Increasing arterial small vessel density was associated with narrower arterial lumen and thicker intima. One potential explanation for this correlation is that in the context of the loss of vascular density as measured by CT scan, the microvasculature that are not lost have different vascular morphology as a subgroup. Another explanation is that the reduction of small vessel density assessed by CT likely reflects vascular pruning resulting from lung tissue destruction rather than from narrowing of small pulmonary arteries, and that these are separated phenomena that might eventually concur in producing pulmonary hypertension in advanced disease stages.

This study demonstrates that CT based imaging findings of loss of distal vasculature are accompanied by loss of vascular cross sectional area on histology. Vascular remodeling has been described as an important component of the development of pulmonary vascular disease (7) including pulmonary arterial hypertension(28, 29). Loss of distal vasculature and changes to the vascular structure assessed using CT imaging have been described in asthma (30), smoking related pulmonary vascular and cardiovascular disease (14, 18, 19), pulmonary arterial hypertension (31, 32) and in CTEPH (33). These changes include proximal arterial dilation, distal loss of vasculature and increased vascular tortuosity as well as overall vascular tree complexity. Understanding the relationship between imaging measurements and histologic measurements will enhance the utility of imaging techniques for quantification of vascular remodeling both in disease progression as well as in response to therapy(34).

One limitation of the presented study is that our cohort consists of subjects with a diagnosis of lung cancer which may have altered underlying anatomic and physiological parameters, although the histologic assessments were performed in areas far from the neoplasm and without apparent tissue distortion. Since lungs were not fixed at a constant inflation, some areas of lung tissue could be collapsed and produce alterations in the measurements of morphometry but to minimize this possibility tissue was distended in PBS previously to fixation. To minimize the effect of this on vascular morphometry, a theoretical diameter of the fully distended artery was calculated by dividing the length of the external elastic lamina by PI as described in a previous study of vascular morphometry(35). Subjects were selected retrospectively, which may have introduced some selection bias into the study. While cohort selections were made in part to minimize heterogeneity in CT acquisition, some variability in image acquisition existed within each cohort. Most patients with COPD used in this study had GOLD stage I or II disease and thus significant COPD burden is not well represented in this data set. Similarly, the burden of emphysema, as assessed by CT scan, was low, and thus there were not significant differences between calculated lung volume and lung volume

adjusted for emphysema. In prior studies the ratio of the small vessel volume to total blood volume has also been proposed as an index of vascular remodeling. This index, however, represents a fundamentally different type of fractional measurement, which while similarly unit-less, can be affected both by loss of distal volume as well as increase in proximal volume, and thus difficult to compare to the histologic measure of vascular density. The vascular density by histology includes veins and arteries because of the difficulty of differentiating them due to vessel size (< 500 μm of diameter) and distortion of sample.

In summary, results of the present study demonstrate that CT assessments of small vessel density reflect the number of small pulmonary vessels, which in smokers and patients with COPD is closely related to the integrity of lung parenchyma. This provides evidence for the utility of imaging based methods of vascular quantification on a macro scale as a marker of vascular pruning on a histologic scale.

Supplementary Material

Refer to Web version on PubMed Central for supplementary material.

Acknowledgments

Authors in this study were supported by Supported by NHLBI grants 5T32HL007633, K23HL136905 (FNR), 1R01HL116931 and 1R01HL116473 (R.S.J.E. and G.R.W); and grant PS0900536 from the Institute of Health Carlos III (ISCIII) (J.A.B), and Agència de Gestió d'Ajuts Universitaris i de Recerca 2017SGR617 (J.A.B.),, Spain.

References:

1. Liebow AA. Pulmonary emphysema with special reference to vascular changes. The American review of respiratory disease. 1959;80(1, Part 2):67–93. Epub 1959/07/01. [PubMed: 13670406]
2. Reid JA, Heard BE. The Capillary Network of Normal and Emphysematous Human Lungs Studied by Injections of Indian Ink. Thorax. 1963;18:201–12. Epub 1963/09/01. [PubMed: 14064613]
3. Kessler R, Faller M, Weitzenblum E, Chaouat A, Aykut A, Ducolone A, Ehrhart M, Oswald-Mammosser M. "Natural history" of pulmonary hypertension in a series of 131 patients with chronic obstructive lung disease. Am J Respir Crit Care Med 2001;164(2):219–24. Epub 2001/07/21. doi: 10.1164/ajrccm.164.2.2006129. [PubMed: 11463591]
4. Chaouat A, Naeije R, Weitzenblum E. Pulmonary hypertension in COPD. Eur Respir J. 2008;32(5): 1371–85. Epub 2008/11/04. doi: 10.1183/09031936.00015608. [PubMed: 18978137]
5. Borden CW, Wilson RH, Ebert RV, Wells HS. Pulmonary hypertension in chronic pulmonary emphysema. Am J Med. 1950;8(6):701–9. Epub 1950/06/01. [PubMed: 15419185]
6. Barr RG. The epidemiology of vascular dysfunction relating to chronic obstructive pulmonary disease and emphysema. Proceedings of the American Thoracic Society. 2011;8(6):522–7. Epub 2011/11/05. doi: 10.1513/pats.201101-008MW. [PubMed: 22052931]
7. Barbera JA. Mechanisms of development of chronic obstructive pulmonary disease-associated pulmonary hypertension. Pulm Circ 2013;3(1):160–4. Epub 2013/05/11. doi: 10.4103/2045-8932.109949. [PubMed: 23662194]
8. Peinado VI, Pizarro S, Barbera JA. Pulmonary vascular involvement in COPD. Chest. 2008;134(4): 808–14. doi: 10.1378/chest.08-0820. [PubMed: 18842913]
9. Voelkel NF, Gomez-Arroyo J, Mizuno S. COPD/emphysema: The vascular story. Pulm Circ. 2011;1(3):320–6. doi: 10.4103/2045-8932.87295. [PubMed: 22140621]
10. Blanco I, Piccari L, Barbera JA. Pulmonary vasculature in COPD: The silent component. Respirology. 2016. doi: 10.1111/resp.12772.

11. Matsuoka S, Washko GR, Dransfield MT, Yamashiro T, San Jose Estepar R, Diaz A, Silverman EK, Patz S, Hatabu H. Quantitative CT Measurement of Cross-sectional Area of Small Pulmonary Vessel in COPD: Correlations with Emphysema and Airflow Limitation(1). Acad Radiol. 2009.
12. Estepar RS, Kinney GL, Black-Shinn JL, Bowler RP, Kindlmann GL, Ross JC, Kikinis R, Han MK, Come CE, Diaz AA, Cho MH, Hersh CP, Schroeder JD, Reilly JJ, Lynch DA, Crapo JD, Wells JM, Dransfield MT, Hokanson JE, Washko GR, Study CO. Computed tomographic measures of pulmonary vascular morphology in smokers and their clinical implications. Am J Respir Crit Care Med. 2013;188(2):231–9. doi: 10.1164/rccm.201301-0162OC. [PubMed: 23656466]
13. Hale KA, Niewoehner DE, Cosio MG. Morphologic changes in the muscular pulmonary arteries: relationship to cigarette smoking, airway disease, and emphysema. The American review of respiratory disease. 1980;122(2):273–8. Epub 1980/08/01. [PubMed: 7416604]
14. Matsuoka S, Washko GR, Yamashiro T, Estepar RS, Diaz A, Silverman EK, Hoffman E, Fessler HE, Criner GJ, Marchetti N, Scharf SM, Martinez FJ, Reilly JJ, Hatabu H, National Emphysema Treatment Trial Research G. Pulmonary hypertension and computed tomography measurement of small pulmonary vessels in severe emphysema. Am J Respir Crit Care Med. 2010;181(3):218–25. doi: 10.1164/rccm.200908-1189OC. [PubMed: 19875683]
15. Santos S, Peinado VI, Ramirez J, Melgosa T, Roca J, Rodriguez-Roisin R, Barbera JA. Characterization of pulmonary vascular remodelling in smokers and patients with mild COPD. Eur Respir J. 2002;19(4):632–8. [PubMed: 11998991]
16. Santos S, Peinado VI, Ramirez J, Morales-Blanhir J, Bastos R, Roca J, Rodriguez-Roisin R, Barbera JA. Enhanced expression of vascular endothelial growth factor in pulmonary arteries of smokers and patients with moderate chronic obstructive pulmonary disease. Am J Respir Crit Care Med. 2003;167(9):1250–6. doi: 10.1164/rccm.200210-1233OC. [PubMed: 12615615]
17. Vlahovic G, Russell ML, Mercer RR, Crapo JD. Cellular and connective tissue changes in alveolar septal walls in emphysema. Am J Respir Crit Care Med. 1999;160(6):2086–92. doi: 10.1164/ajrccm.160.6.9706031. [PubMed: 10588633]
18. Rahaghi FN, Wells JM, Come CE, De La Bruere IA, Bhatt SP, Ross JC, Vegas-Sanchez-Ferrero G, Diaz AA, Minhas J, Dransfield MT, San Jose Estepar R, Washko GR, and the CI. Arterial and Venous Pulmonary Vascular Morphology and Their Relationship to Findings in Cardiac Magnetic Resonance Imaging in Smokers. J Comput Assist Tomogr. 2016;40(6):948–52. doi: 10.1097/RCT.0000000000000465. [PubMed: 27636250]
19. Washko GR, Nardelli P, Ash SY, Vegas Sanchez-Ferrero G, Rahaghi FN, Come CE, Dransfield MT, Kalhan R, Han MK, Bhatt S, Wells JM, Aaron CP, Diaz AA, Ross JC, Cuttica MJ, Labaki WW, Querejeta Roca G, Shah AM, Young K, Kinney GL, Hokanson JE, Agusti A, San Jose Estepar R, Investigators CO. Arterial Vascular Pruning, Right Ventricular Size and Clinical Outcomes in COPD. Am J Respir Crit Care Med. 2019. doi: 10.1164/rccm.201811-2063OC.
20. Schneider CA, Rasband WS, Eliceiri KW. NIH Image to ImageJ: 25 years of image analysis. Nat Methods. 2012;9(7):671–5. [PubMed: 22930834]
21. Ross JC, Estepar RS, Diaz A, Westin CF, Kikinis R, Silverman EK, Washko GR. Lung extraction, lobe segmentation and hierarchical region assessment for quantitative analysis on high resolution computed tomography images. Medical image computing and computer-assisted intervention : MICCAI International Conference on Medical Image Computing and Computer-Assisted Intervention. 2009;12(Pt 2):690–8.
22. Estepar RS, Ross JC, Krissian K, Schultz T, Washko GR, Kindlmann GL. Computational Vascular Morphometry for the Assessment of Pulmonary Vascular Disease Based on Scale-Space Particles. Proceedings / IEEE International Symposium on Biomedical Imaging: from nano to macro IEEE International Symposium on Biomedical Imaging. 2012:1479–82. Epub 2012/01/01. doi: 10.1109/ISBI.2012.6235851.
23. Kindlmann GL, San Jose Estepar R, Smith SM, Westin CF. Sampling and visualizing creases with scale-space particles. IEEE transactions on visualization and computer graphics. 2009;15(6):1415–24. Epub 2009/10/17. doi: 10.1109/TVCG.2009.177. [PubMed: 19834216]
24. Nardelli PLM, Møller CB, Andersen A-SH, Jørgensen AS, Østergaard LR, San José Estépar R. Accurate Measurement of Airway Morphology on Chest CT Images. Lecture Notes In Computer Science 2018;11040:335–47.

25. Matsuoka S, Yamashiro T, Washko GR, Kurihara Y, Nakajima Y, Hatabu H. Quantitative CT assessment of chronic obstructive pulmonary disease. Radiographics. 2010;30(1):55–66. doi: 10.1148/rg.301095110. [PubMed: 20083585]
26. Madani A, Zanen J, de Maertelaer V, Gevenois PA. Pulmonary emphysema: objective quantification at multi-detector row CT--comparison with macroscopic and microscopic morphometry. Radiology. 2006;238(3):1036–43. doi: 10.1148/radiol.2382042196. [PubMed: 16424242]
27. Nardelli P, Jimenez-Carretero D, Bermejo-Pelaez D, Washko GR, Rahaghi FN, Ledesma-Carbayo MJ, Estepar RSJ. Pulmonary Artery-Vein Classification in CT Images Using Deep Learning. IEEE transactions on medical imaging. 2018. doi: 10.1109/TMI.2018.2833385.
28. Chaudhary KR, Taha M, Cadete VJ, Godoy RS, Stewart DJ. Proliferative Versus Degenerative Paradigms in Pulmonary Arterial Hypertension: Have We Put the Cart Before the Horse? Circ Res. 2017;120(8):1237–9. doi: 10.1161/CIRCRESAHA.116.310097. [PubMed: 28408451]
29. Vonk-Noordegraaf A, Marcus JT, Holverda S, Roseboom B, Postmus PE. Early changes of cardiac structure and function in COPD patients with mild hypoxemia. Chest. 2005;127(6):1898–903. Epub 2005/06/11. doi: 10.1378/chest.127.6.1898. [PubMed: 15947300]
30. Ash SY, Rahaghi FN, Come CE, Ross JC, Colon AG, Cardet-Guisasola JC, Dunican EM, Bleecker ER, Castro M, Fahy JV, Fain SB, Gaston BM, Hoffman EA, Jarjour NN, Mauger DT, Wenzel SE, Levy BD, San Jose Estepar R, Israel E, Washko GR, Investigators S. Pruning of the Pulmonary Vasculature in Asthma. The Severe Asthma Research Program (SARP) Cohort. Am J Respir Crit Care Med. 2018;198(1):39–50. doi: 10.1164/rccm.201712-2426OC. [PubMed: 29672122]
31. Helmberger M, Pienn M, Urschler M, Kullnig P, Stollberger R, Kovacs G, Olschewski A, Olschewski H, Balint Z. Quantification of tortuosity and fractal dimension of the lung vessels in pulmonary hypertension patients. PLoS One. 2014;9(1):e87515. doi: 10.1371/journal.pone.0087515. [PubMed: 24498123]
32. Moledina S, de Bruyn A, Schievano S, Owens CM, Young C, Haworth SG, Taylor AM, Schulze-Neick I, Muthurangu V. Fractal branching quantifies vascular changes and predicts survival in pulmonary hypertension: a proof of principle study. Heart. 2011;97(15):1245–9. doi: 10.1136/hrt.2010.214130. [PubMed: 21303796]
33. Rahaghi FN, Ross JC, Agarwal M, Gonzalez G, Come CE, Diaz AA, Vegas-Sanchez-Ferrero G, Hunsaker A, San Jose Estepar R, Waxman AB, Washko GR. Pulmonary vascular morphology as an imaging biomarker in chronic thromboembolic pulmonary hypertension. Pulm Circ. 2016;6(1):70–81. doi: 10.1086/685081. [PubMed: 27162616]
34. Rahaghi FN, Winkler T, Kohli P, Nardelli P, Marti-Fuster B, Ross JC, Radhakrishnan R, Blackwater T, Ash SY, de La Bruere I, Diaz AA, Channick RN, Harris RS, Washko GR, San Jose Estepar R. Quantification of the Pulmonary Vascular Response to Inhaled Nitric Oxide Using Noncontrast Computed Tomography Imaging. Circ Cardiovasc Imaging. 2019;12(1):e008338. doi: 10.1161/CIRCIMAGING.118.008338. [PubMed: 30632391]
35. Barbera JA, Riverola A, Roca J, Ramirez J, Wagner PD, Ros D, Wiggs BR, Rodriguez-Roisin R. Pulmonary vascular abnormalities and ventilation-perfusion relationships in mild chronic obstructive pulmonary disease. Am J Respir Crit Care Med. 1994;149(2 Pt 1):423–9. doi: 10.1164/ajrccm.149.2.8306040. [PubMed: 8306040]

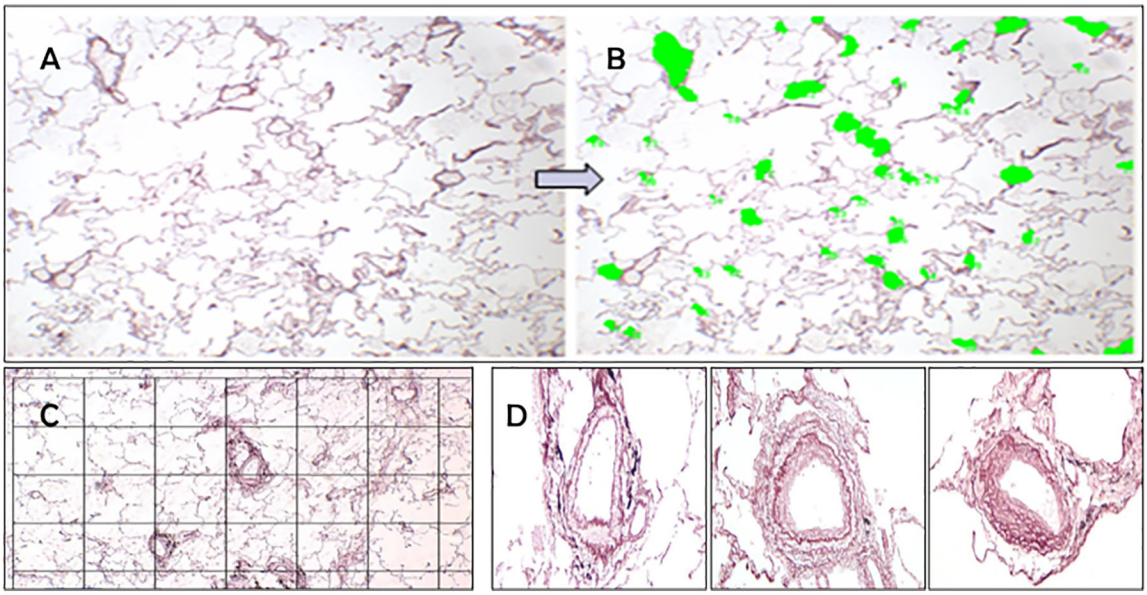

Figure 1.

Photograph of a section prepared from excised lung tissue of patients undergoing lung resection for a tumor **(A).** Vessels were identified manually and colored in. The cross sectional area of vessels less than 500μ were added and divided by the entire field of view to derive the Histologic Vessel Cross Sectional Area (%hist-VCSA)(**B**). To measure the proportion of tissue structures, a grid point was placed and points corresponding to alveolar septa, vessels and bronchiole were identified(**C**). The thickness of the wall, wall components and lumen were measured from individual arteries **(D)**. Example artery from a nonsmoker (left panel in **D)**, one from a subject with GOLD II COPD (middle panel in **D)** and one from GOLD III disease (right panel in **D)** are shown here.

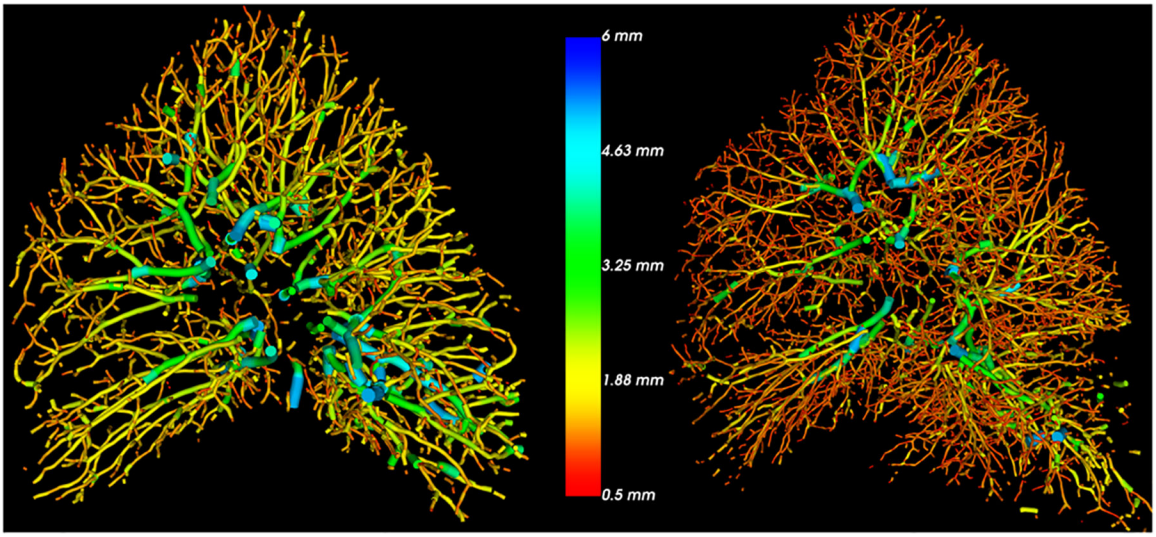

Figure 2.

Examples of 3D vascular reconstruction in two subjects both with GOLD II COPD. Imaging of the subject to the left shows proximal dilation and loss of distal vasculature as compared to the subject on the right. The color indicates the radius of the vessel with red coloring representing smaller vessels. On histology, the subject on the left has a lower %hist-VCSA (6.3 versus 8.6). (VCSA: Vascular cross-sectional area)

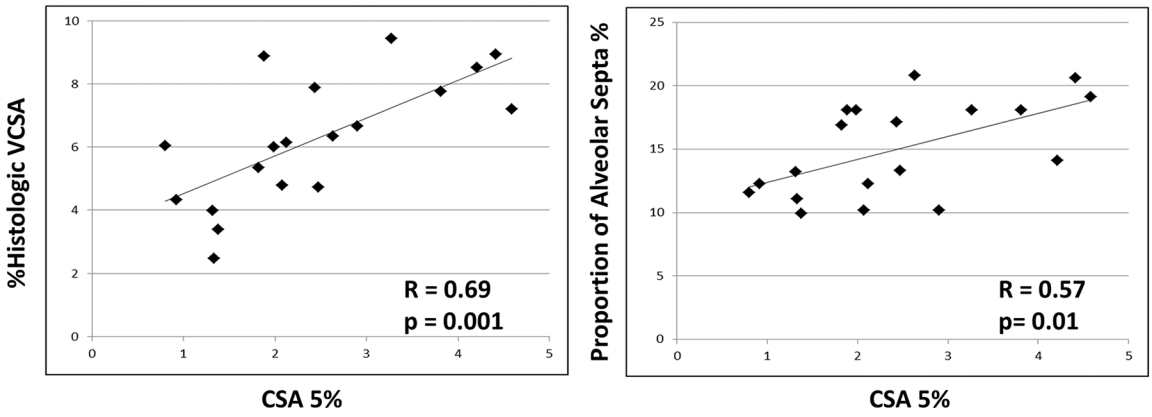

Figure 3.

Summary of results from the 2D analysis showing a correlation between cross-sectional area of vessels of less than 5mm^2 assessed by CT scan and histologic metrics of small vessel (diameter <500 μm) density (%hist-VCSA) as well as the estimated proportion of alveolar septa. (VCSA: Vascular Cross Sectional Area).

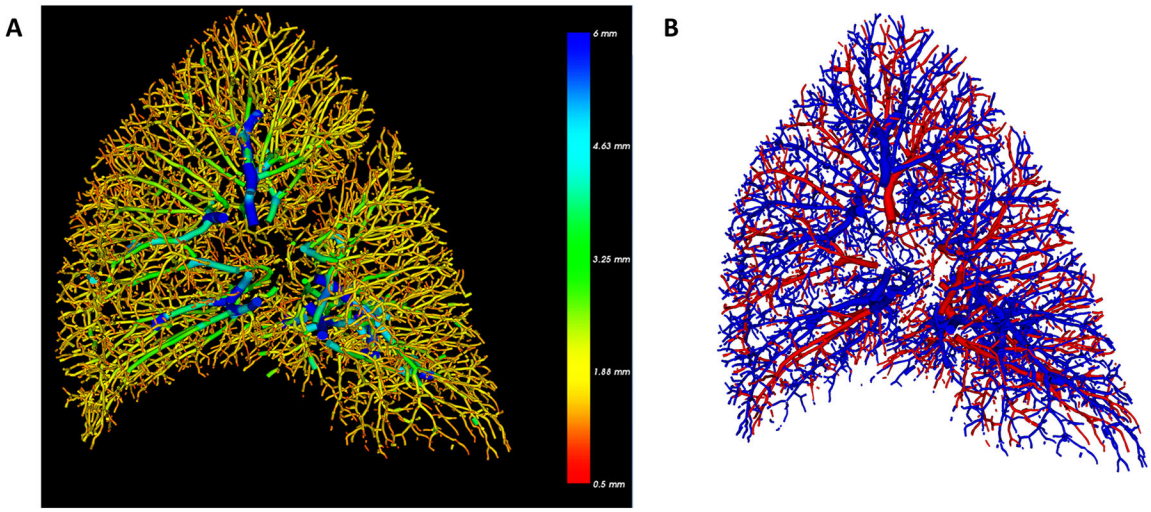

Figure 4.

Example of 3D reconstruction of a right lung (A) where blue indicates larger (radius of 6mm and cross sectional area of ~110mm^2) and red indicates smaller vessels with radius of 0.5mm and cross sectional area of 0.8mm^2 (B) shows the subsequent automated arterial and venous segmentation where blue denotes arteries and red denotes veins.

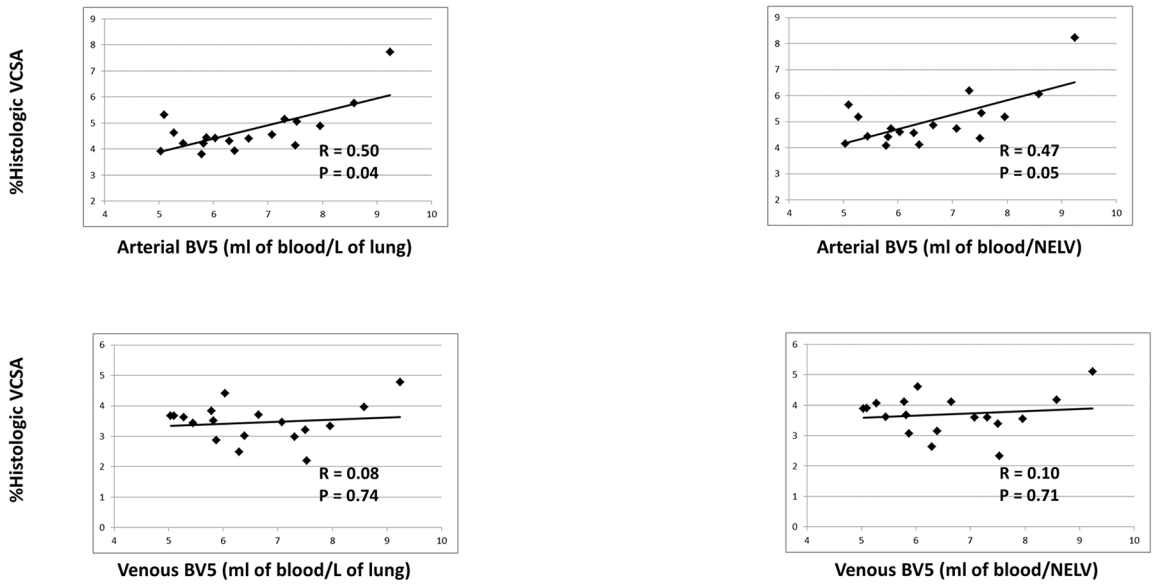

Figure 5.

Relationship between estimated vascular volume in arterial BV5 and venous BV5 small vessels normalized by lung volume or by tissue volume and histologic metrics of small vessel (diameter <500 μm) density (%hist-VCSA) and the estimated proportion of alveolar septa. Correlation coefficients are nonparametric (Spearman). (BV5: blood vessel volume in vessels less than $5mm^2$ in cross sectional area; VCSA: vascular cross sectional area; NELV: non-emphysematous lung volume)

Table 1:

Demographics and Clinical Characteristics of the Two Analyzed Cohorts

	All Subjects N = 37	**Cohort For 3D Reconstruction N = 18**	**Cohort For 2D Analysis N = 19**
Gender (F/M)	21/16	12/6	9/10
Age (years)	66 (12)	68 (14)	64 (15)
BMI	27 (6)	26 (4)	28 (5)
Smokers (N)	30	16	14
Smoking Exposure (packs-year)	40 (45)	40 (37)	45 (56)
FEV_1/FVC (%)	68 (12)	65 (7)	73 (11)
FEV_1 (%pred)	77 (20)	71 (18)	85 (19)
FVC (%pred)	85 (20)	85 (23)	84 (16)
TLC (%pred)	94 (17)	88 (22)	95 (12)
DLCO (%pred)	74 (18)	65 (13)	77 (16)
PaO_2 (mmHg)	83 (12)	83 (6)	78 (14)
COPD (N, %)	21 (57%)	13 (72%)	8 (42%)

*Represented as medians and interquartile Range

Table 2:

Histologic Measures of the Two Analyzed Cohorts

	All Subjects N = 37	Cohort For 3D Reconstruction N = 18	Cohort For 2D Analysis N = 19
Estimated proportion of lung structures			
Alveolar space (%)	81 (8.8)	83 (6.1)	80 (11)
Alveolar septa (%)	14 (6.8)	14 (5.6)	14 (6.1)
Vessels (%)	4.2 (2.8)	4.1 (1.4)	4.4 (4.2)
Bronchi (%)	0.5 (0.7)	0.5 (0.7)	0.0(0.7)
Cross-sectional area of vessels <500 μm diameter (% total area)			
	6.3 (2.2)	6.3 (1.7)	6.1 (3.1)
Morphometry of pulmonary muscular arteries			
External diameter (μm)	277 (96.0)	266 (93.7)	278 (97.5)
Lumen (% vessel area)	41 (16)	41 (9)	41 (18)
Intima (% vessel area)	30 (11)	31 (12)	28 (10)
Muscularis (% vessel area)	24 (7)	25 (6)	23 (9)

*Represented as medians and interquartile Range

Table 3:

CT Based Imaging Measures.

Measures in the 2D cohort (N = 19)	
2D CSA5 %	**2.12 (1.49)**
Measures in the 3D Cohort (N = 18)	
%LAA-950	0.3 (1.4)
Lung Volume (L)	4.5 (1.4)
Lung Mass (g)	889 (212)
Non Emphysematous Lung Volume (L)	4.25 (1.24)
Measures of Vascular Volume	
BV5 (mL)	34.9 (16.1)
TBV (mL)	78.5 (28.1)
BV5/LV	7.9 (0.85)
TBV/LV	16.9 (2.7)
BV5/NELV	8.3 (13.7)
TBV/NELV	18.1 (3.0)
Arterial BV5 (mL)	19.9 (8.6)
Arterial BV5/LV	4.4 (0.8)
Arterial BV5/NELV	4.7 (0.9)

* Represented as medians and interquartile ranges.

BV5: Blood vessel volume in vessels with cross-sectional area of of less than $5mm^2$. **TBV**: Total blood vessel volume. **LV**: Lung Volume. **NELV**: Non Emphysematous Lung Volume.